

Structure and dynamics of $\text{Cl}^-(\text{H}_2\text{O})_{20}$ clusters: The effect of the polarizability and the charge of the ion

Lalith Perera and Max L. Berkowitz

Department of Chemistry, University of North Carolina, Chapel Hill, North Carolina 27599

(Received 23 December 1991; accepted 24 February 1992)

The effect of the polarizability and the sign of the ionic charge were studied in $\text{Cl}^-(\text{H}_2\text{O})_{20}$ clusters using molecular dynamics computer simulation technique. From our simulations we concluded that the reduction in the ionic polarizability did not significantly change the structure and dynamics of the $\text{Cl}^-(\text{H}_2\text{O})_{20}$ cluster, but the inversion of the sign of the ionic charge produced a large effect. The energetic considerations helped us to understand why Cl^- is located on the surface of the cluster. By being on the surface the anion permits the creation of the hydrogen bonded network between water molecules and that lowers the total energy of the cluster. Simulations with the inverted sign of the ionic charge correspond to that with a hypothetical " Cl^+ " ion which is similar in size and polarizability to a Cs^+ ion. The dynamical structures and the quenched structures of $\text{Cl}^+(\text{H}_2\text{O})_{20}$ clusters are compared with the idealized structure of the $\text{Cs}^+(\text{H}_2\text{O})_{20}$ cluster proposed recently [A. Selinger and A. W. Castleman, Jr., *J. Phys. Chem.* **95**, 8442 (1991)].

I. INTRODUCTION

Recent experimental and theoretical studies performed on aqueous clusters display a rich dynamical and structural behavior that characterizes these systems.¹⁻¹¹ Some experiments indicate that water structures of well-defined geometry may enclose ions, such as NH_4^+ (Ref. 4), H_3O^+ (Refs. 5, 6), OH^- (Ref. 7), and Cs^+ (Ref. 8). Of special interest are clusters where 20 water molecules are encaging the ion. It was proposed that the enhanced stability of these clusters is due to the formation of a pentagonal dodecahedron which surrounds the ion.^{6,8} In contrast, other experiments indicate that water structure in a cluster of solvating anions such as Cl^- may not be that regular.⁹ Moreover, some of the cluster structures in this case are rather unexpected. For example, in our recent molecular dynamics study of the $\text{Cl}^-(\text{H}_2\text{O})_{14}$ cluster we obtained a rather interesting result: in this cluster the anion is partially solvated, it is located on the surface of the cluster.¹⁰ Similar conclusions on the character of solvation were also reached in the studies performed on electrons solvated in water clusters.^{11,12}

The immediate question that comes to one's mind is why the Cl^- ion is situated on a surface of the cluster? Is that due to the large polarizability of the Cl^- ion, or is it due to the sign of the ionic charge? To answer these questions we performed three molecular dynamics simulations. In all three simulations the system was composed of 20 water molecules and one ion. In the first simulation we considered the dynamics of 20 water molecules and one Cl^- ion; in the second simulation we studied the structure and dynamics of a cluster of 20 water molecules and one Cl^+ ion, i.e., in this system the ion/water interaction was described by the same set of parameters as in the previous simulation, except the charge on the Cl^- ion was changed from -1 to $+1$. By doing this, we were able to investigate how the sign of the ionic charge

affects the solvation of the ion. It is appropriate to mention here that the Cl^+ ion is very similar to the Cs^+ ion, since the sizes and polarizabilities of the two ions are very similar. (The ionic radius of Cl^- is 1.81 Å, while the ionic radius of Cs^+ is 1.7 Å. The polarizabilities of Cl^- and Cs^+ are 3.25 Å³ and 2.56 Å³, respectively.)

In order to study how the large polarizability of the Cl^- ion influences the dynamics and the structure of the cluster, we reduced the value of Cl^- polarizability in the third simulation. In what follows, the Cl^- ion with a reduced polarizability is referred to as the Cl_{TP}^- ion.

II. METHODS

In our previous work we have shown that the inclusion of many-body interaction effects in the molecular dynamics simulation of ion/water clusters is essential in order to reproduce the correct energetics of the clusters.¹⁰ Therefore in these simulations we again used the SPCE/POL potential model^{13,14} which includes many-body effects. In this model the water molecule is assumed to have three charges placed at the positions of two hydrogens and the oxygen. The Lennard-Jones center is placed on the oxygen site. The OH distance in the model is 1 Å and the HOH angle is 109.47°. Three polarizable centers are placed at each atomic site in water. The ion in this model is considered to be a point charge placed at a Lennard-Jones center. Additionally a polarization center is also placed at the same location.

The total energy of the system is given by the following expression:

$$U_{\text{tot}} = U_{\text{el}} + U_{\text{LJ}} + U_{\text{pol}} + U_{3\text{ body}}, \quad (1)$$

where

$$U_{\text{el}} = \sum_{i < j} \frac{q_i q_j}{r_{ij}} \quad (2)$$

is the sum of all Coulomb interactions between all i and j charge sites and

$$U_{\text{LJ}} = \sum_{\alpha < \beta} [A_{\alpha\beta}/r_{\alpha\beta}^{12} - C_{\alpha\beta}/r_{\alpha\beta}^6] \quad (3)$$

is the sum of the Lennard-Jones interactions between α and β Lennard-Jones sites. The polarization energy is obtained from the expression¹⁵

$$U_{\text{pol}} = \sum_{i < j} \boldsymbol{\mu}_i \cdot \mathbf{T}_{ij} \cdot \boldsymbol{\mu}_j - \sum_i q_i \sum_j \frac{\boldsymbol{\mu}_j \cdot \mathbf{r}_{ij}}{|\mathbf{r}_{ij}|^3} + \sum_i \frac{\mu_i^2}{2\alpha_i}, \quad (4)$$

where α_i is the polarizability, μ_i is the induced dipole at the polarizable i th center, and \mathbf{r}_{ij} is the distance vector from site i to site j . The values of the induced dipoles at the polarizable centers are calculated self-consistently using the following relationships:

$$\boldsymbol{\mu}_i = \alpha_i \mathbf{E}_i, \quad (5)$$

$$\mathbf{E}_i = \mathbf{E}_i^0 - \sum_j \mathbf{T}_{ij} \cdot \boldsymbol{\mu}_j, \quad (6)$$

where \mathbf{E}_i is the total electrostatic field at the i th center and \mathbf{E}_i^0 is the field due to permanent charges. The dipole tensor \mathbf{T}_{ij} in Eq. (6) is

$$\mathbf{T}_{ij} = 1/r_{ij}^3 [\mathbf{I} - 3\mathbf{r}_{ij}\mathbf{r}_{ij}/r_{ij}^2]. \quad (7)$$

The potential energy due to the three-body exchange repulsion of the ion-water trimer is expressed in terms of ion-oxygen distances r_{ij} and r_{ik} , and the oxygen-oxygen distance r_{jk}

$$U_{3\text{ body}} = B \exp(-\beta r_{ij}) \exp(-\beta r_{ik}) \exp(-\gamma r_{jk}), \quad (8)$$

where B , β , and γ are parameters. The potential parameters of the SPCE/POL model are given in Table I.

A. Molecular dynamics

We used molecular dynamics computer simulations to investigate the structure and dynamics of small clusters made up of one ion and 20 water molecules. Equations of motion were solved using the Verlet algorithm.¹⁶ The geometries of the water molecules at their equilibrium values were constrained through the Shake procedure.¹⁷ To solve

self-consistent Eqs. (5) and (6) an iterative approach was used. The iterations were continued until the root mean square of the difference in the induced dipoles between successive iterations was less than 0.001 D/atom. The self-consistency was usually achieved in seven steps of iteration.

Each cluster was initially equilibrated for more than 20 ps followed by 500 ps of the production run. The time step of the trajectory has been kept at 1 fs and the total linear and angular momenta of the system were removed. During the trajectory calculations the energy was conserved within the 5th significant digit.

All the trajectory calculations were done in the micro-canonical ensemble at temperatures around 200 K. The observed temperature fluctuations were around 30 K. The temperature of the cluster was chosen to be high enough to eliminate possible trapping of the cluster in a certain configuration for a very long time. We attempted to perform some molecular dynamics simulations of our clusters at 300 K, but observed the evaporation of water molecules at this temperature.

III. RESULTS AND DISCUSSIONS

Since the net translational and rotational motions of the center of mass were absent in our simulations, we used the distance from the ion to the origin as an index of the cluster solvation. If a cluster is completely solvated, this distance, as well as the distance to the center of mass of the water molecules should approach zero. The two distances, shown in Figs. 1(a), 1(b), and 1(c) also provide information on

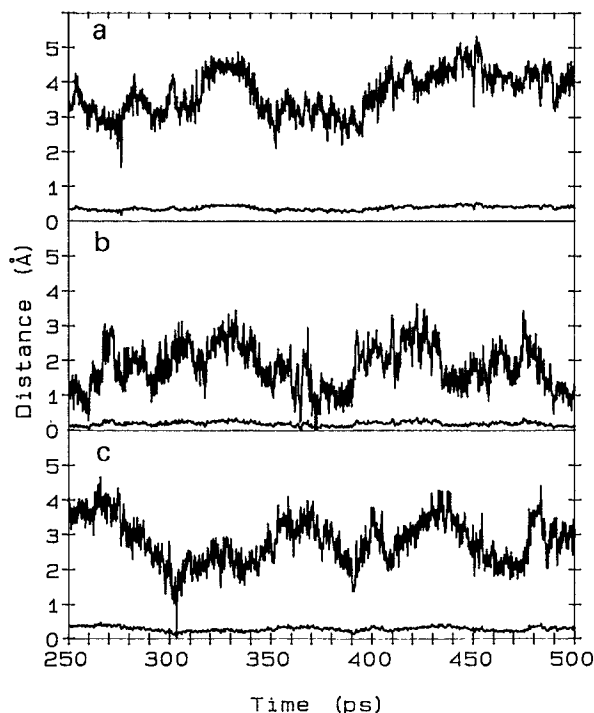


FIG. 1. The time dependence of the distance from the center of mass to the ion [(a) Cl⁻, (b) "Cl⁺" and (c) Cl_{ip}⁻]. The time dependent distance between the center of mass of the water molecules and the whole cluster is also shown and it corresponds to the curves which are close to zero.

TABLE I. Potential energy parameters, charges, and polarizabilities used in the SPCE/POL model. $B * 10^6$ (kcal/mol) = 0.80, β (Å⁻¹) = 2.25, γ (Å⁻¹) = 0.25.

	$A * 10^{-5}$ (kcal Å ¹² /mol)	C (kcal Å ⁶ /mol)
O-O	6.37	627.95
O-ion	37.90	1373.84
	$q(e)$	α (Å ³)
O	-0.73	0.465
H	0.365	0.135
Cl ⁻	-1.0	3.25
Cl ⁺	1.0	3.25
Cl _{ip} ⁻	-1.0	0.0025

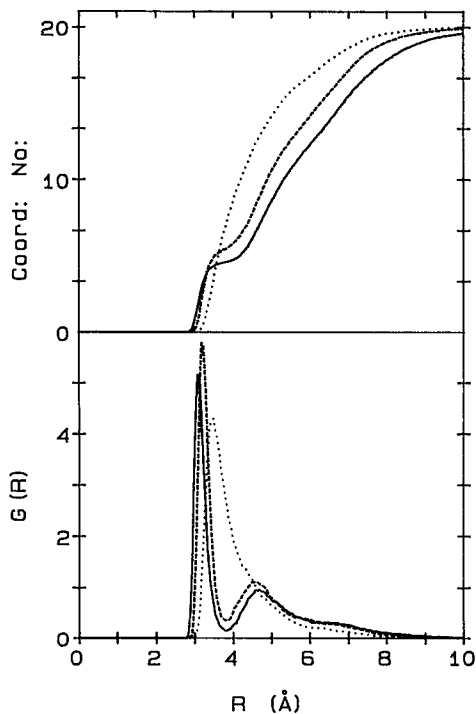


FIG. 2. Calculated ion-oxygen radial distribution functions (bottom) and the running coordination numbers (top). The solid line is for Cl^- -O rdf, the dotted line is for Cl^+ -O rdf and the dashed line is for Cl_p^- -O rdf.

whether the cluster is symmetric when the solvation takes place. From comparison of Figs. 1(a), 1(b), and 1(c) we can see that the most solvated ion is Cl^+ .

To gain more insight into the structure of the clusters we calculated the ion-water radial distribution functions (rdf),

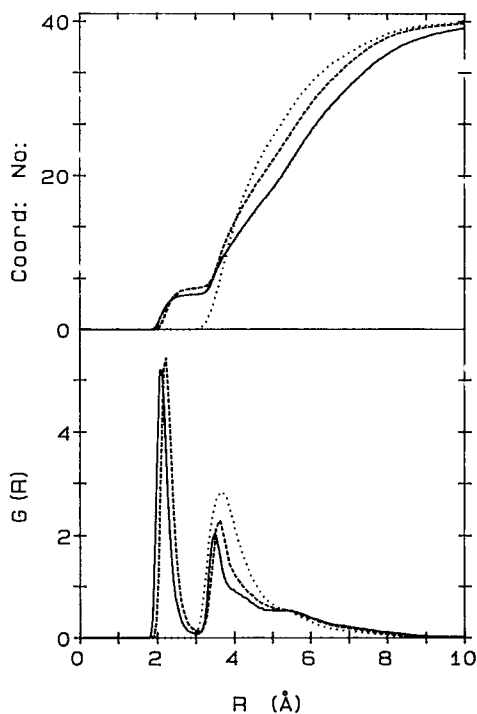


FIG. 3. Calculated ion-hydrogen radial distribution functions (bottom) and the running coordination numbers (top). Solid line is for Cl^- -H rdf, dotted line is for Cl^+ -H rdf and the dashed line is for Cl_p^- -H rdf.

which are represented in Figs. 2 and 3. Figure 2 displays the ion-oxygen rdf and Fig. 3 displays the ion-hydrogen rdf. For Cl^- /water cluster the first maximum in ion-oxygen rdf is at $r = 3.05 \text{ \AA}$, the coordination number of the ion is 4.5. However, for a Cl^- ion solvated in bulk water at 300 K these values are correspondingly 3.2 \AA and 6.1 (Ref. 14). The reduction of the polarizability of the Cl^- ion produces a shift in the position of the first maximum of ion-oxygen rdf towards a larger value of the distance and an increase of the coordination number to the value of 5.5. In the case of the Cl^- ion the radial distribution functions clearly show that the solvation shell consists of a primary shell and a broad secondary shell. This is not so in the case of the Cl^+ ion, for which only one broad shell of solvation is observed. There are two peaks in Cl^- -hydrogen rdf, corresponding to two different positions of hydrogens: The first peak is due to the hydrogens that are oriented towards the ion, the second is due to hydrogens that are pointing away from the ion. In the case of the Cl^+ -hydrogen rdf the picture is quite different: Only one broad peak is present which has a shoulder starting at $\sim 5.7 \text{ \AA}$. It is very interesting that the plot of coordination numbers indicates that there are ~ 10 hydrogen atoms beyond this distance. These hydrogens may be considered to be external to the cluster and may be available for bonding in the type of titration experiments performed by Castleman's group.⁶ Note that in the idealized structure proposed by Castleman *et al.*^{6,8} there are also 10 hydrogens available for bonding. Also notice here that the peaks of Cl^+ -O rdf and Cl^+ -H rdf appear at approximately the same distance, although one normally expects to see the cation-oxygen peak appear at shorter distances than the cation-hydrogen peak.

Additional information on the structure of the clusters and the solvation pattern around the ion can be obtained from the angular distribution function (adf), which is displayed in Fig. 4. In this figure we show the distribution for the angles between the vector connecting the ion and the water oxygen and the vector connecting the ion with the center of mass of water molecules that are the nearest neigh-

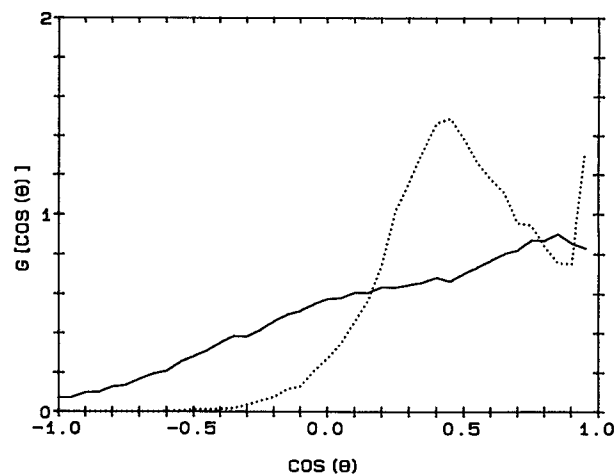


FIG. 4. Calculated angular distribution functions for $\text{Cl}^-(\text{H}_2\text{O})_{20}$ (dotted line) and $\text{Cl}^+(\text{H}_2\text{O})_{20}$ (solid line) clusters. The definition of the angle Θ is given in the text.

bors of the ion. Thus for Cl^- ion only waters that have their oxygens closer than 3.9 Å from the ion are taken into account. For the Cl^+ ion we considered all the water molecules that have their oxygens below 5.7 Å, where, as we mentioned above, the beginning of a slight shoulder in the water-ion rdf can be observed. As we can see from Fig. 4, the behavior of the adf is different for the Cl^- and Cl^+ ions. The adf for the Cl^- ion clearly shows that the ion is solvated on one side, while water molecules can be found at any angle around the Cl^+ ion. Note that even for the Cl^+ ion the solvation is not homogeneous, pointing out that also in this case the ion may be found near the surface of the cluster.

The analysis of the total energy of the clusters and its components can help us to understand the structural and dynamical behavior of the clusters. The total potential energy of the cluster can be written as a sum of two components: water-ion and water-water interaction energies, i.e.,

$$U_{\text{tot}} = U_{\text{i-w}} + U_{\text{w-w}}. \quad (9)$$

In its turn, the water-water interaction energy can be further divided in to the electrostatic ($U_{\text{el}}^{\text{w-w}}$), Lennard-Jones ($U_{\text{LJ}}^{\text{w-w}}$), and polarization ($U_{\text{pol}}^{\text{w-w}}$) components. In addition to these components the water-ion interaction energy also includes the three-body term ($U_{3-b}^{\text{i-w}}$). In Table II(a) we display the time averaged values of all the components for the water-ion and water-water interaction energies. In part (b) of Table II we present the total values of the electrostatic, Lennard-Jones, polarization, and three-body energies and finally in part (c) of Table II we present the total potential energies and the two components of this energy which are given by Eq. (9).

As we can see from Table II, the cluster with Cl^- ion is the most energetically stable one. It is interesting to notice

that the contributions of water-water and water-ion energies into the total energy are nearly the same in this case. Also notice the rather large contribution of the polarization energy. Even in the case of a $\text{Cl}_{\text{rp}}^-/\text{water}$ cluster the polarization energy is substantial, mainly due to the polarizability of the water molecules. The reduction of the polarizability on the Cl^- ion results in a slightly weaker ion-water interaction. This is consistent with the slight change in the shape of the radial distribution functions. For the cluster with the Cl^+ ion the major contribution to the energy comes from the water-water interaction. The ion-water interaction in this case is weaker compared to the one observed in the Cl^-/water cluster, in spite of the fact that the cluster is more solvated. The strong ion-water interaction observed in a Cl^- water cluster is due to the close proximity of water hydrogens to the ion. This is not the case for the Cl^+/water cluster, where, as the radial distributions show, oxygens and hydrogens are on the average at the same distance away from the ion.

To get a better understanding of the relationship between the cluster structure and its dynamics we have analysed some snapshots of cluster configurations. Figures 1(a)–1(c) were used as guidelines in our analysis. As Fig. 1(a) indicates, the Cl^- ion is expected to be located on the surface of the water cluster during the whole trajectory. This was confirmed by direct observations of cluster structures. Some representative structures of a $\text{Cl}^-(\text{H}_2\text{O})_{20}$ cluster are displayed in Fig. 5. Figure 1(b) indicates that dynamical transitions between fully solvated and partially solvated structures occur in the case of the Cl^+ cluster. This is indeed revealed from the snapshots, which are displayed in Fig. 6. While the ion is on the surface of the cluster at $t = 332.9$ ps it is solvated at $t = 377.1$ ps and again moves to the surface at

TABLE II. (a) Components of the potential energy (in kJ/mol) for different $\text{X}(\text{H}_2\text{O})_{20}$ clusters. [The subscripts rp, min, and id are used to represent the reduced polarizability of the Cl^- ion, the lowest minimum energy structure found during the quenching of 250 samples and the idealized structure according to Castleman *et al.* (Refs. 6 and 8), respectively.] (b) Energy components as in Eq. (1). (c) Total potential energies and their major components as in Eq. (9).

	Cl^-	Cl^+	Cl_{rp}^-	Cl_{min}^-	Cl_{min}^+	Cl_{id}^+
(a)						
$U_{\text{el}}^{\text{w-w}}$	− 593.4	− 644.1	− 562.1	− 776.4	− 804.5	− 772.0
$U_{\text{LJ}}^{\text{w-w}}$	205.8	227.9	188.7	318.5	284.8	223.6
$U_{\text{pol}}^{\text{w-w}}$	− 74.5	− 125.9	− 83.1	− 120.8	− 173.4	− 120.9
$U_{\text{el}}^{\text{i-w}}$	− 360.7	− 256.6	− 372.8	− 376.0	− 250.8	− 154.0
$U_{\text{LJ}}^{\text{i-w}}$	53.1	11.8	37.4	64.0	8.1	− 5.4
$U_{\text{pol}}^{\text{i-w}}$	− 132.1	− 52.0	− 78.0	− 162.9	− 55.0	− 56.2
$U_{3-b}^{\text{i-w}}$	8.0	5.0	7.2	8.9	6.9	5.3
(b)						
U_{el}	− 954.1	− 900.7	− 934.9	− 1152.4	− 1055.3	− 926.0
U_{LJ}	258.9	239.7	226.1	382.5	292.9	218.2
U_{pol}	− 206.6	− 177.9	− 161.1	− 283.7	− 228.4	− 177.1
U_{3-b}	8.0	5.0	7.2	8.9	6.9	5.3
(c)						
$U_{\text{w-w}}$	− 462.1	− 542.1	− 456.5	− 578.7	− 693.1	− 669.3
$U_{\text{i-w}}$	− 431.7	− 291.8	− 406.2	− 466.0	− 290.8	− 210.3
U_{tot}	− 893.8	− 833.8	− 862.9	− 1044.7	− 983.9	− 879.6

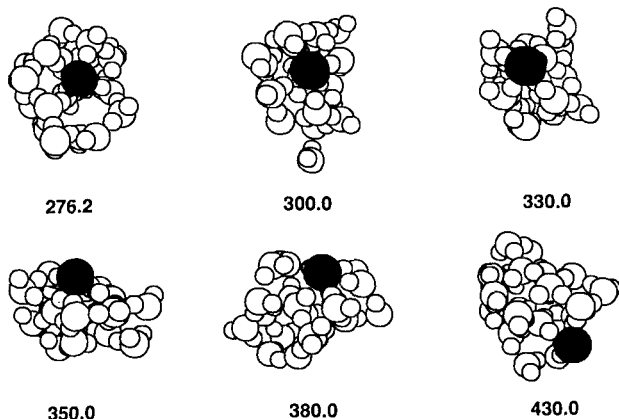


FIG. 5. Snapshots taken from a trajectory of $\text{Cl}^-(\text{H}_2\text{O})_{20}$ cluster. Time (in ps) at which the configuration appeared is given below each snapshot.

$t = 422.4$ ps. The structure at $t = 377.1$ ps is close to the proposed idealized structure which, according to Castleman and co-workers, surrounds the Cs^+ ion.⁸ For comparison we present the two structures in Fig. 7. As we can see from this figure, the dynamical structure for the Cl^+ /water cluster represents a torus made out of 20 water molecules with the center occupied by the ion. The idealized structure proposed by Castleman *et al.*^{6,8} has a higher symmetry of a pentagonal dodecahedron.

A. Minimum energy structures

To compare the energetics of the idealized $\text{Cl}^+(\text{H}_2\text{O})_{20}$ cluster structure with the energetics of the other stable structures, we have to find these other stable structures. For this purpose 250 configurations, selected at 1 ps interval from the trajectories of the clusters with Cl^- and Cl^+ ions were quenched. Figures 8 and 9 represent the energy components of these quenched structures which correspond to different local minima. A salient feature observed from these figures is the presence of a broad distribution of energies, pointing to the existence of a large manifold of local

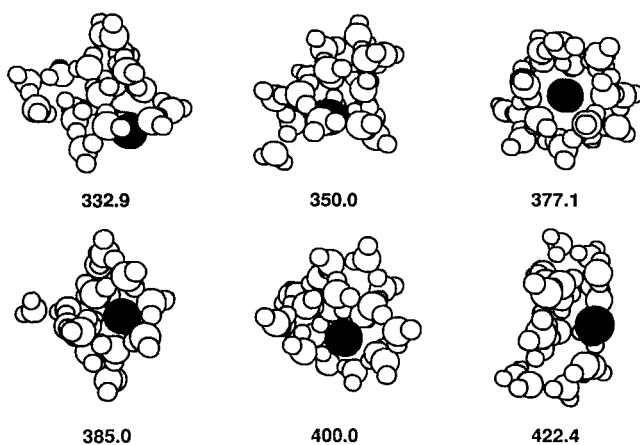


FIG. 6. Snapshots taken from a trajectory of $\text{Cl}^+(\text{H}_2\text{O})_{20}$ cluster.

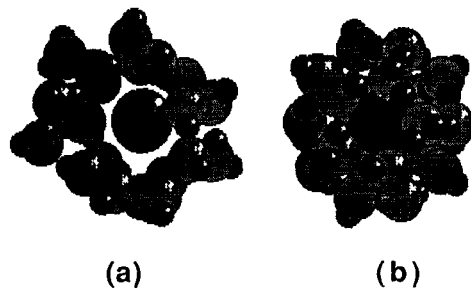


FIG. 7. (a) A configuration of $\text{Cl}^+(\text{H}_2\text{O})_{20}$ cluster (at $t = 377.1$ ps); (b) The idealized structure proposed by Castleman *et al.*^{6,8}

minimum structures. We also observe from the figures that the distribution of water-ion interaction energy for the quenched Cl^- /water cluster is broader than the one for the Cl^+ /water cluster, indicating that the clusters with the Cl^- ion are less symmetrical. This is consistent with the conclusions we have reached previously.

For the lowest energy configurations, we display the energies and their components in parts (a)–(c) of Table II in order to compare them with the average energies of the dynamical clusters. As we can see from the tables and Fig. 8 the water-water interaction energy of the most energetically stable structure of the Cl^- /water cluster falls short of the maximum possible water-water interaction energy, observed in quenched structures, but it is not very far from the latter. The ion-water interaction energy for this cluster is right in the middle of the observed values for this component of the total energy. The structure corresponding to this minimum energy configuration of the quenched $\text{Cl}^-(\text{H}_2\text{O})_{20}$ cluster is given in Fig. 10(a).

For the most stable configuration of the cluster with a Cl^+ ion, the water-water interaction energy is at its lowest value, while the water-ion energy is close to the highest value observed for this interaction. The structure of this most stable configuration of the $\text{Cl}^+(\text{H}_2\text{O})_{20}$ cluster is displayed

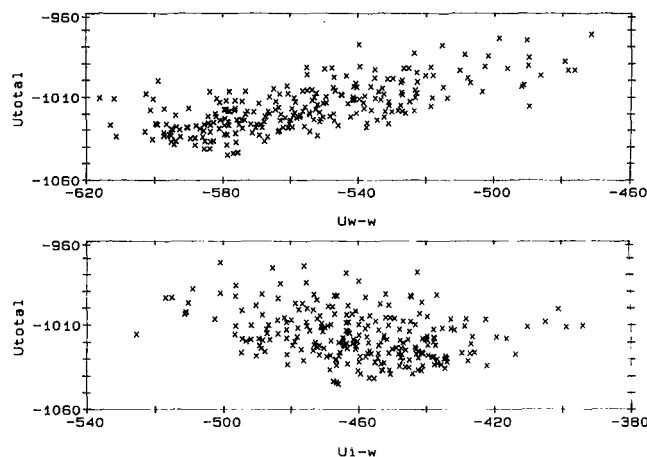


FIG. 8. U_{total} vs U_{w-w} (top) and U_{total} vs U_{1-w} (bottom) for the quenched $\text{Cl}^-(\text{H}_2\text{O})_{20}$ configurations.

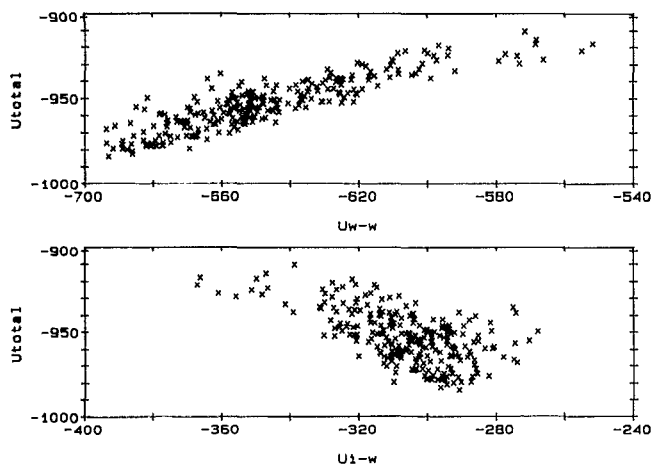


FIG. 9. U_{tot} vs $U_{\text{w-w}}$ (top) and U_{tot} vs $U_{\text{l-w}}$ (bottom) for the quenched $\text{Cl}^+(\text{H}_2\text{O})_{20}$ configurations.

in Fig. 10(b). While the dynamical configuration has a shape of a torus, we can see that the most energetically stable configuration has a form of a “baseball glove” with the ion representing the “ball.”

The observed minimum energy structures from Figs. 10(a) and 10(b) and a comparison of the energetics of these structures with the data from Table II indicate that the stability of the quenched structures is achieved by lowering the water–water interaction energy. We also observe that the energy of the idealized structure is about 100 kJ/mol higher than the energy of the most stable quenched structure.

IV. CONCLUSIONS

At the outset of the work we raised the question why the Cl^- ion is partially solvated by small clusters of water mole-

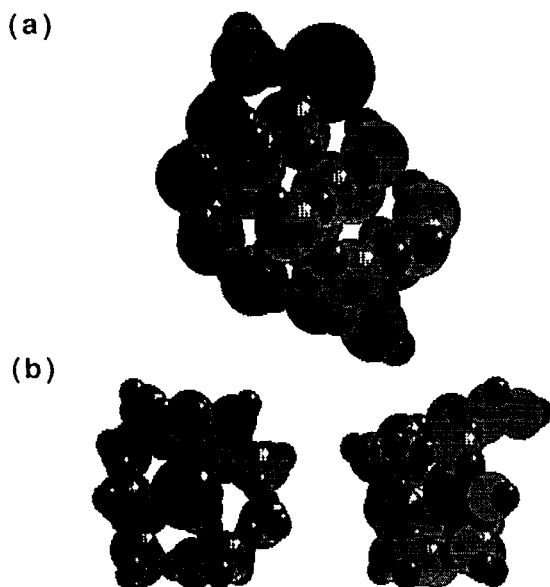


FIG. 10. The structures corresponding to lowest energy configurations obtained in quenching of (a) $\text{Cl}^-(\text{H}_2\text{O})_{20}$ and (b) $\text{Cl}^+(\text{H}_2\text{O})_{20}$ clusters. The right hand side structure in (b) is the side view (obtained after 90° rotation) of the left hand side structure.

cules. To check if that was due to a large ionic polarizability we have investigated the structure and dynamics of clusters where the polarizability of the ion was reduced. To see the effect of the ionic charge we investigated the structure and dynamics of clusters where the sign of the ionic charge was inverted. From our simulations we conclude that the reduction in the ionic polarizability does not significantly change the structure and dynamics of the $\text{Cl}^-(\text{H}_2\text{O})_{20}$ cluster, but the sign inversion of the ionic charge produces a large effect. While the Cl^- ion prefers to be situated on the cluster surface, the Cl^+ ion undergoes dynamical transitions in the cluster, moving from its surface to a location where the solvation is more complete. The energetic considerations helped us to understand why Cl^- is located on the surface of the cluster. By being on the surface the anion permits the creation of the hydrogen bonded network between water molecules that lowers the total energy of the cluster.

When the solvation of the ion is at its maximum in the $\text{Cl}^+(\text{H}_2\text{O})_{20}$ cluster, the cluster has a shape of a torus. This structure is topologically similar to the pentagonal dodecahedron, which is the proposed idealized structure for the $\text{Cs}^+(\text{H}_2\text{O})_{20}$ cluster. Nevertheless, by quenching some selected configurations obtained from the dynamical simulations, we observed that the minimum energy structure has the shape of a baseball glove, and is about 100 kJ/mol lower in energy than the idealized structure. In the present work, our major goal was to study the effect of the ionic charge inversion on the structure and dynamics of the Cl^- /water clusters and not the structure and dynamics of Cs^+ /water clusters. But, since Cl^+ and Cs^+ ions have similar sizes and polarizabilities, we believe that our conclusions reached about the $\text{Cl}^+(\text{H}_2\text{O})_{20}$ cluster can be applied as well to a $\text{Cs}^+(\text{H}_2\text{O})_{20}$ cluster.

It is interesting to compare our results with the results obtained from other computer simulations performed on inhomogeneous aqueous systems, for example, with the results from the simulations that study the structure and dynamics of the ion and water when the ion is close to the water/vapor interface.^{18–20} The results from the simulations^{18–20} show that water molecules at the interface interact with the anion more favorably than with the cation. We have reached a similar conclusion in our simulations performed on small aqueous clusters. But contrary to the observations we made in small clusters, it was observed in Refs. 18–20 that ions keep their solvation shell at the water/vapor interface. It is also known^{18–20} that the ions are negatively adsorbed on the water/vapor surface, i.e., it costs energy to move the ions from the bulk to the surface. That means that for the large size clusters we should observe the complete solvation of the anion. The question that remains to be answered is how large is large?

ACKNOWLEDGMENTS

This work was supported by a grant from the Office of Naval Research. The simulations were performed on the Cray-YMP supercomputer at North Carolina Supercomputer Center and on a Convex Supercomputer at UNC com-

putational center. We are grateful to the referee for the careful reading of the manuscript. Work of B. Price and Dr. I. Vaisman on the visualization of clusters is greatly appreciated.

- ¹ P. L. M. Plummer and T. S. Chen, *J. Phys. Chem.* **87**, 4190 (1983).
- ² I. P. Buffey, W. Byers Brown, and H. A. Gebbie, *Chem. Phys. Lett.* **148**, 281 (1988).
- ³ P. W. Fowler, C. M. Quinn, and D. B. Redmond, *J. Chem. Phys.* **95**, 7678 (1991).
- ⁴ H. Shinohara, U. Nagashima, H. Tanaka, and N. Nishi, *J. Chem. Phys.* **83**, 4183 (1985).
- ⁵ X. Yang and A. W. Castleman, Jr., *J. Am. Chem. Soc.* **111**, 6845 (1989).
- ⁶ S. Wei, Z. Shi, and A. W. Castleman, Jr., *J. Chem. Phys.* **94**, 3268 (1991).
- ⁷ X. Yang and A. W. Castleman, Jr., *J. Phys. Chem.* **94**, 8500 (1990).
- ⁸ A. Selinger and A. W. Castleman, Jr., *J. Phys. Chem.* **95**, 8442 (1991).
- ⁹ D. R. Zook and E. P. Grimsrud, *Int. J. Mass Spectrom. Ion Proc.* **107**, 293 (1991).
- ¹⁰ L. Perera and M. L. Berkowitz, *J. Chem. Phys.* **95**, 1954 (1991).
- ¹¹ R. N. Barnett, U. Landman, and A. Nitzan, *J. Chem. Phys.* **89**, 2242 (1988).
- ¹² R. N. Barnett, U. Landman, G. Makov, and A. Nitzan, *J. Chem. Phys.* **93**, 6226 (1990).
- ¹³ J. Caldwell, L. X. Dang, and P. A. Kollman, *J. Am. Chem. Soc.* **112**, 9145 (1990).
- ¹⁴ L. X. Dang, J. E. Rice, J. Caldwell, and P. A. Kollman, *J. Am. Chem. Soc.* **113**, 2481 (1991).
- ¹⁵ L. Perera and F. G. Amar, *J. Chem. Phys.* **90**, 7354 (1989).
- ¹⁶ L. Verlet, *Phys. Rev.* **159**, 98 (1967).
- ¹⁷ J. P. Ryckaert, G. Ciccotti, and H. J. C. Berendsen, *Comput. Phys.* **23**, 327 (1977).
- ¹⁸ M. A. Wilson, A. Pohorille, and L. R. Pratt, *Chem. Phys.* **129**, 209 (1989).
- ¹⁹ M. A. Wilson and A. Pohorille, *J. Chem. Phys.* **95**, 6005 (1991).
- ²⁰ I. Benjamin, *J. Chem. Phys.* **95**, 3698 (1991).